# Stability of Amazon Backscatter at C-band: Spaceborne Results from ERS-1/2 and RADARSAT-1

**RK Hawkins[†], E Attema[‡], R Crapolicchio*, P Lecomte*, Josep Closa[♥], PJ Meadows[+], and SK Srivastava[††]**

[†]Canada Centre for Remote Sensing, 588 Booth St, Ottawa, K1A 0Y7, Canada;
Email: robert.hawkins@ccrs.nrcan.gc.ca

[‡]European Space Agency, ESTEC, PO Box 299, 2200 AG Noordwijk, The Netherlands;
Email: eattema@estec.esa.nl

*European Space Agency, ESRIN/PCS, 00044 Frascati, Italy; Email: rcrapoliccho@esrin.esa.it, plecomte@esrin.esa.it, Josep.Closa@esrin.esa.it

♥ SERCO Srl /ESA/ESRIN, 00044 Frascati, Italy; Email: Josep.Closa@esrin.esa.it

[+]Marconi Research Centre, West Hanningfield Rd, Chelmsford, Essex, CME 8HN, United Kingdom;
Email: peter.meadows@gecm.com

[††]Canadian Space Agency, 6767 Route de l'aéroport, Saint Hubert, Québec, Canada;
Email: satish.srivastava@space.gc.ca

## ABSTRACT

This paper looks at the question of the temporal and spatial stability of the Amazon rainforest as a distributed target calibration source. The Amazon rainforest has been established by a number of investigators as a useful means of determining the in-orbit antenna pattern of spaceborne SAR and scatterometers. It was used for ERS-1 and ERS-2, J-ERS-1, and RADARSAT-1 providing a large isotropic backscattering reference over a wide range of incidence angle. In this paper, we look at a long series of results from ERS and RADARSAT to examine the temporal and spatial stability of this target class. These properties are supported by a simple radar signature model.

In any radar measurement, uncompensated variation in the sensor may be included with changes in target backscatter. Results from independent measurements from precision transponders are used to assess the size and characteristics of these inherent systematic variations before discussing the implications of the Amazon backscatter measurements.

The implications of the results for future missions are also explored.

## INTRODUCTION

The Amazon rainforest is a vast area comprising over $3x10^6$ km$^2$ located along the equator, mostly (2/3) in Brazil but extending into Peru, Colombia and Ecuador. It consists of a high, dense canopy stretching to approximately 30 m although there is considerable diversity in types and stages [1,2]. Biomass ranges from 100 to 300 tons/ha with annual precipitation, approximately 3 m. This region is popularly understood as the source of ~30% of the oxygen flux, a storehouse of biodiversity and a natural indicator of climate and other ecological changes.

To the incident radar frequencies used in remote sensing satellites and many airborne systems which operate at X, C and L-band, most of the scattered radiation is from the crown area and tends to have a slow incidence angle, $\theta_{inc}$, variation which can be characterized by the relation:

$$\gamma = \text{constant} = \sigma^o / \cos\theta_{inc} = \beta^o \tan\theta_{inc} \qquad \textbf{(1)}$$

Here $\gamma$, $\sigma^o$, and $\beta^o$ are forms of the backscattering coefficient and radar brightness used to define the scattering properties of a distributed target [3]. This property and small temporal variation, first noted with Seasat and Skylab [2], together with a number of logistic advantages which include the large areal extent and low relief of the area (<200 m) make the use of the Amazon forest a favoured site for the determination of in-flight antenna patterns for the synthetic aperture radars (SAR) and scatterometers: Seasat [4], ERS-1 [5], ERS-2, RADARSAT [6], JERS-1 and Sir-C [7]. In these instances, property (1) is used to invert the radar equation allowing a determination of the relative antenna pattern in the elevation plane. The details of that inversion depend on the normalization used in the

SAR processor and other implementation factors of the system.

Despite the fact that the Amazon basin constitutes a wide area of relatively high homogeneity, care is taken in practise to assure that any local departures are handled by appropriate statistical filtering [8] when antenna pattern shapes are derived. Fig. 1 is a J-ERS-1 composite of the entire Amazon basin [9] showing the homogeneity and variability of the region.

Table 1: Characteristics of operational instruments

| **Instrument** | **Freq** (GHz) | **Pol** | $\theta_{inc}$ | **Res**† (m) |
|---|---|---|---|---|
| ERS-1/2 SAR | 5.30 | VV | 19-27$^o$ | 25 |
| ERS-1/2 Scatterometer | 5.30 | VV | 18-59$^o$ | 50000 |
| J-ERS-1 | 1.275 | VV | 36-41$^o$ | 18 |
| RADARSAT-1 | 5.30 | HH | 10-59$^o$ | 25 |

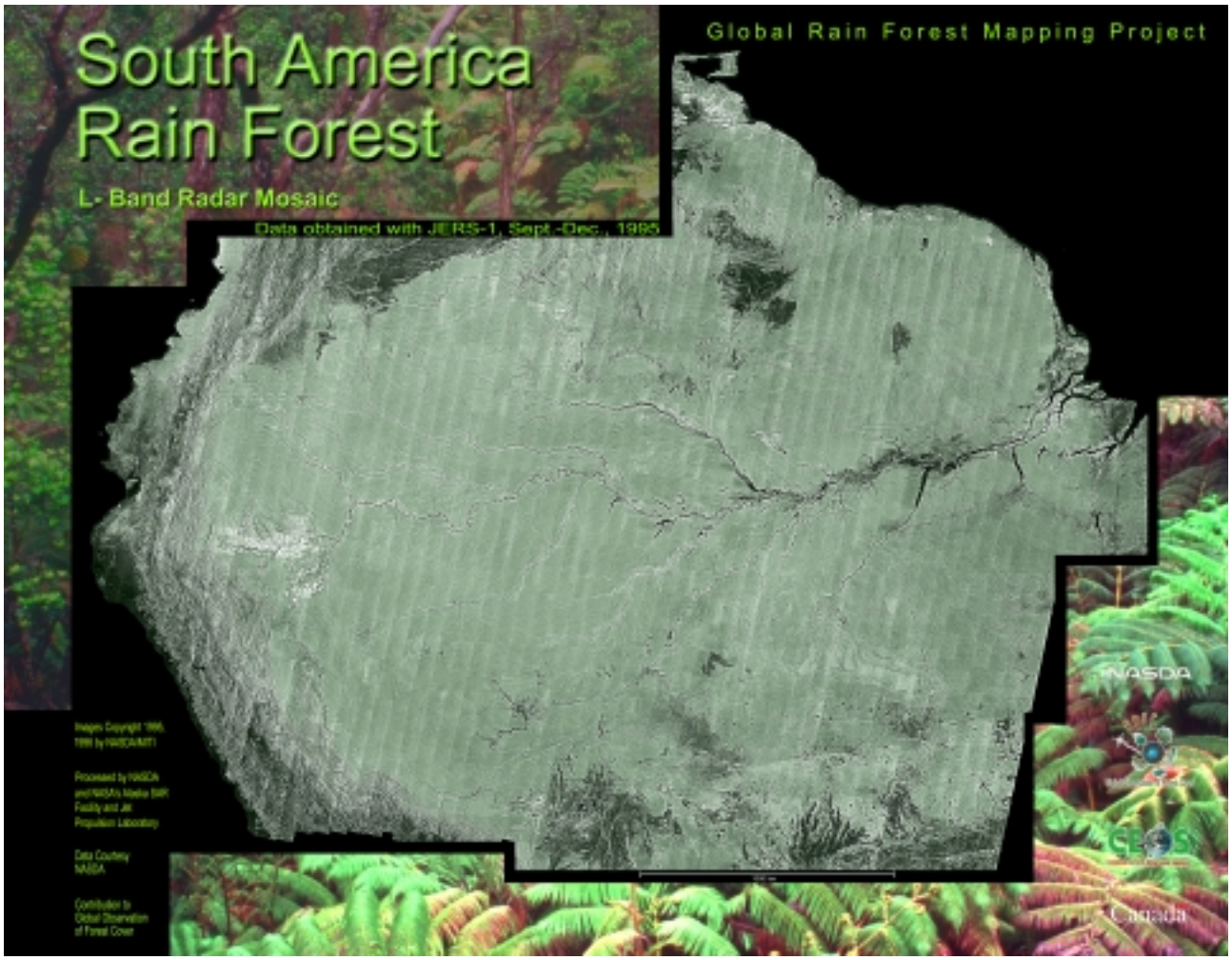


Fig. 1: J-ERS-1 mosaic of the Amazon basin. Descending passes from over 60 swaths are combined in the mosaic comprised of approximately 2000 individual scenes.

Operational satellites have had an opportunity to repeatedly view the region and should be able to provide some sort of seasonal if not longer term basis. This is particularly true of J-ERS-1, ERS-1/2, and RADARSAT-1. Table 1 gives a summary of some overall parameters of these instruments germane to this discussion.

We note differences in frequency, polarization, and incidence angles. For this study, we will restrict our focus to the C-band instruments. In the sections below, we comment on the scattering theory which leads to property (1) and then go on to discuss the results from ERS and RADARSAT.

† Resolution here is of a typically processed product for this analysis.

## MICROWAVE SIGNATURE MODEL OF DENSE FOREST

Because the microwave dielectric constant of dry vegetative matter is much smaller than the dielectric constant of water, and because a canopy (even a dense forest) is composed of more than 99% air by volume, a radar signature model for vegetation canopies has been proposed in which the canopy is represented by a water cloud whose droplets are held in place by the vegetative matter [10]. Applying radiative transfer theory to this model, the radar backscattering coefficient per unit projected area, $\gamma$ for dense forests simply depends on the biomass, B (tons/ha), incidence angle and two empirical parameters, C and D. These parameters depend on a number of physical quantities such as target structure, radar wavelength, and polarisation. According to the cloud model, the equation for $\gamma$ can be written as

$$\gamma = C\left[1-\exp\left(\frac{BD}{\cos\theta_{inc}}\right)\right] \qquad \textbf{(2)}$$

Fig. 2 shows that this simple model nicely predicts the well known saturation of the radar echo for higher values of biomass as well as the smooth variation with incidence angle already expressed in (1). In the example shown, C=0.23 and D=0.05, are values considered appropriate for C-band, VV polarisation.

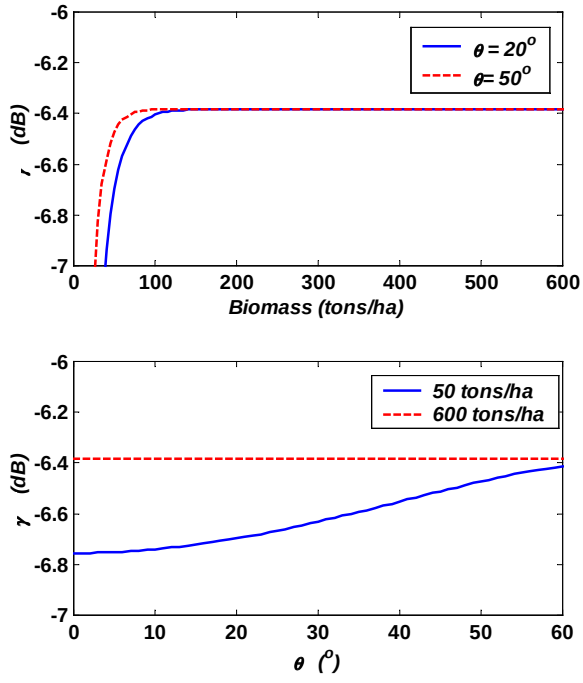


Fig. 2: Dense forest model of $\gamma$ as a function of biomass and incidence angle

For the biomass appropriate to the rainforest, this theory suggests asymptotic (constant) behaviour for the backscatter with biomass and incidence angle.

## ERS-1/2 SCATTEROMETER RESULTS

Some of the most complete data sets from the Amazon rainforest come from the ERS-1/2 scatterometers [11] which have been in continuous operation since 1991. The instrument has three side looking beams with a swath of 500 km with diversity in azimuth look direction. Ongoing monitoring of the area [12] located between 2.5°N and 5.0°S and 62.5°W and 75.0°W occurs with weekly synopses for each of the beams in ascending and descending geometries. Fig. 3 shows a monthly synopsis and Fig. 4, an associated histogram providing weekly statistics from approximately the same time frame. From these figures, we note:

- The three beams appear to be measuring slightly different properties but differ by as little as 0.1 dB.
- There is significant (> 1 dB) spatial variation over the test region.
- Ascending (night) and descending (day) passes also show strongly varying spatial distributions.

Fig. 5 shows the variation of the weekly means from each of the ERS-2 scatterometer beams for the period January, 1996 to April 1999. We note:

- Both ascending and descending passes show an annual cycle with amplitude approximately 0.15 dB modulating more noise like variations about 0.05 dB. (The large step in the early part of the data stream is due to a calibration adjustment.)
- The annual variation is thought to be geophysical in nature since it has been shown to be uncorrelated with annual variations in the antenna temperature (2° C) [13]. Similar annual variations with ERS-1 *could not* be correlated with specific rainfall events at Benjamin Constant [16]. This result is not necessarily at odds with ERS-1 scatterometer results recently published [14] which show *strong* seasonal correlation between accumulative precipitation over a period of about 30 days. These authors have shown variations as much as 0.5 dB during 1993 from a Guyanian rainforest test site of 50 × 50 km. More typical global RMS variations [15], determined from ERS-1, are 0.59 dB.

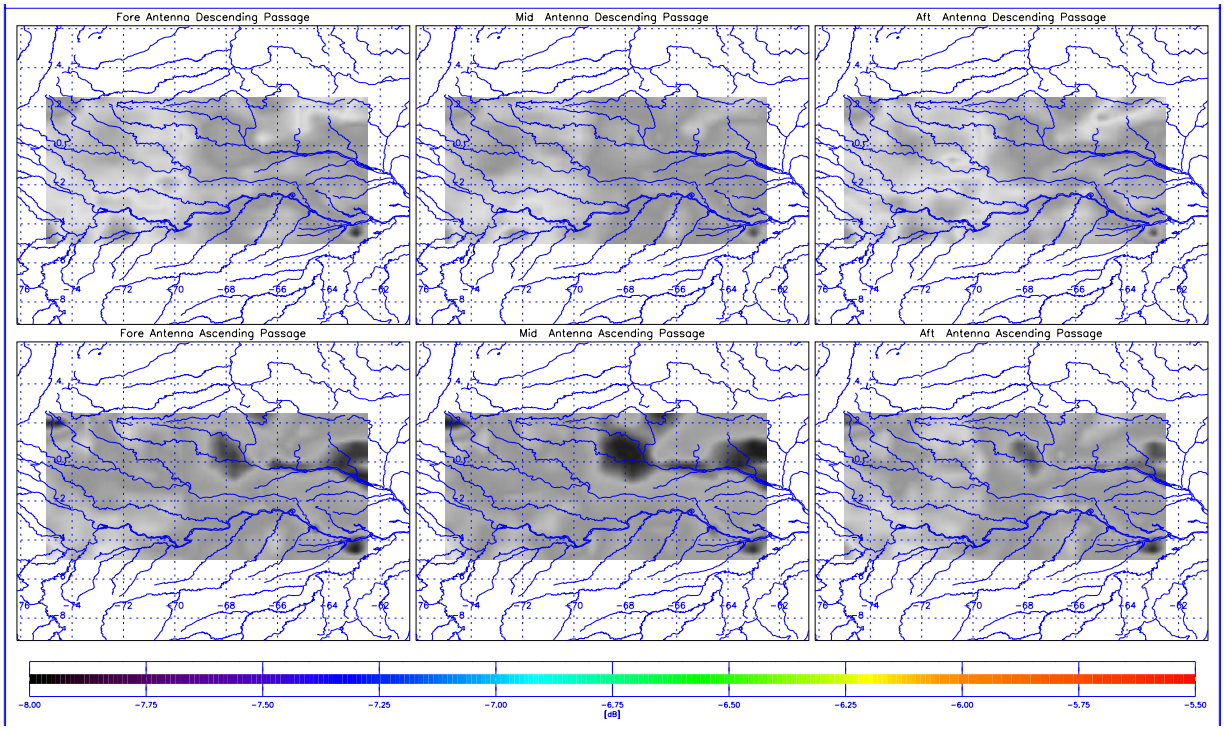


Fig. 3: ERS-2 windscatterometer monthly synopsis $\gamma$ image of Amazon basin March 13 to April 18, 1999

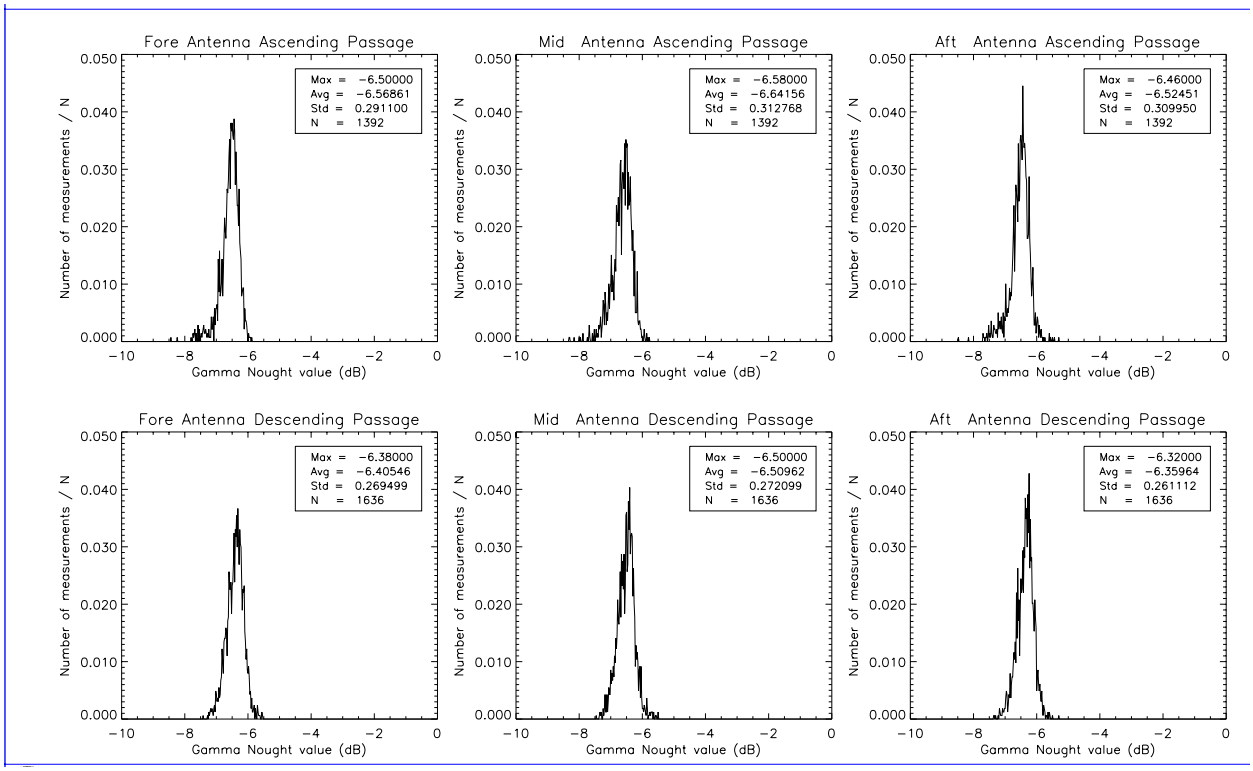


Fig.4: Weekly $\gamma$ histogram synopsis from ERS-2 from April 12 to April 18, 1999

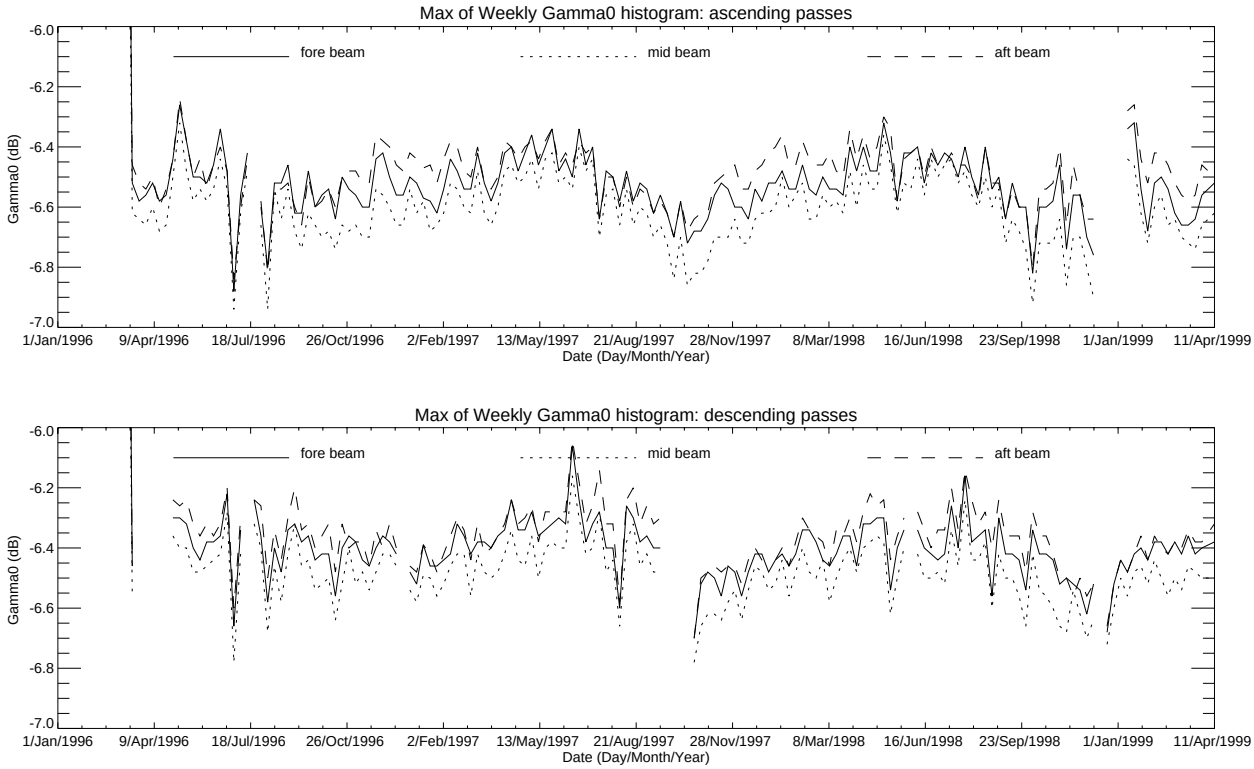


Fig. 5: History of weekly $\gamma$ maxima from ERS-2 scatterometer from Jan 1996 to April 1999

ERS Scatterometer Stability

The ERS scatterometer was calibrated [16] using the Amazon to derive antenna patterns and transponders to derive the absolute levels. The small differences in the mean levels in the three beams are believed related to the measurements biases introduced in the calibration. Compared to the ERS SAR, these instruments have had less attention paid to their calibration [17], and relatively fewer measurements [18] have been taken during the commissioning phase of the instrument.

In Fig. 6, features of the ESA scatterometer transponder calibration data for the *forebeam* are shown. as the *DGCF* (differential gain correction factor) defined as:

$$DGCF = \frac{\text{Measured RCS}}{\text{Actual RCS}} \qquad (3)$$

Variation in the *DGCF* reflects uncertainty in the instrument calibration for an individual scene at the incidence angle of the point target measurement. It is a measure of the total number of interrelated uncertainties including S/C roll, recovery of the point target impulse response, processing as well as systematic drifts in both the calibrator and the radar. We can only discuss the variation in Amazon data in the wider context of the stability shown with these point target references since they are a measure of our ability to characterize the overall performance of the system. At the top, is the dependence of *DGCF* across the 10 scatterometer beam segments showing individual measurements; in the middle, is a time history irrespective of beam; and, at the bottom a histogram of that data measuring a RMS variation of 0.20 dB. This is our best direct knowledge of the scatterometer stability and is very much better than the system specification of 0.7 dB.

The data are combined across the swath to obtain this statistic to compare with the weekly synoptic averages discussed above. We believe that this figure represents a pessimistic estimation of the scatterometer stability because of limitations in the instrumentation and techniques employed. Indeed, data from the Greenland ice cap [19] have shown stabilities better than 0.1 dB over an extended time. Fig. 7 shows the temporal backscatter stability in the interior of Greenland [20].

Given these results, it is likely that, of the three instruments studied in this paper, the ERS scatterometer has the most sensitivity to small changes in the backscatter of the Amazon. The measurements are however for larger area footprints than the 'imaging' SAR sensors.

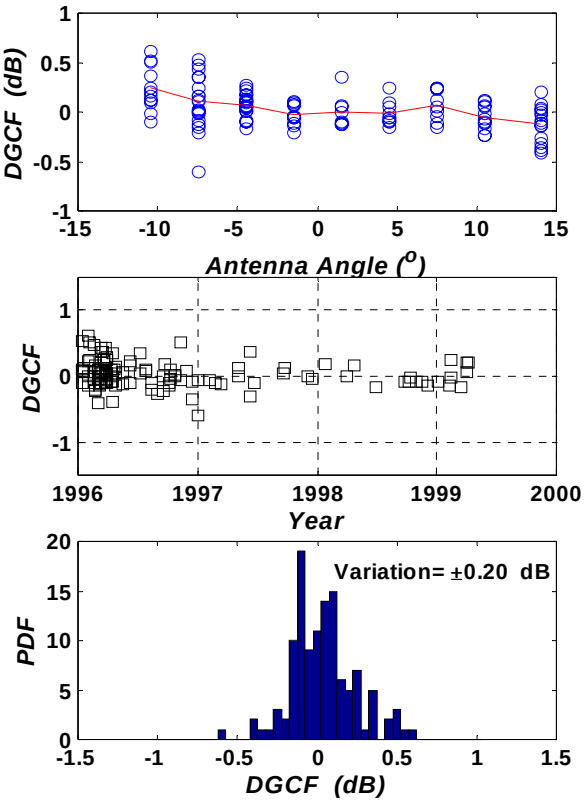


Fig. 6: ERS-2 scatterometer forebeam transponder results

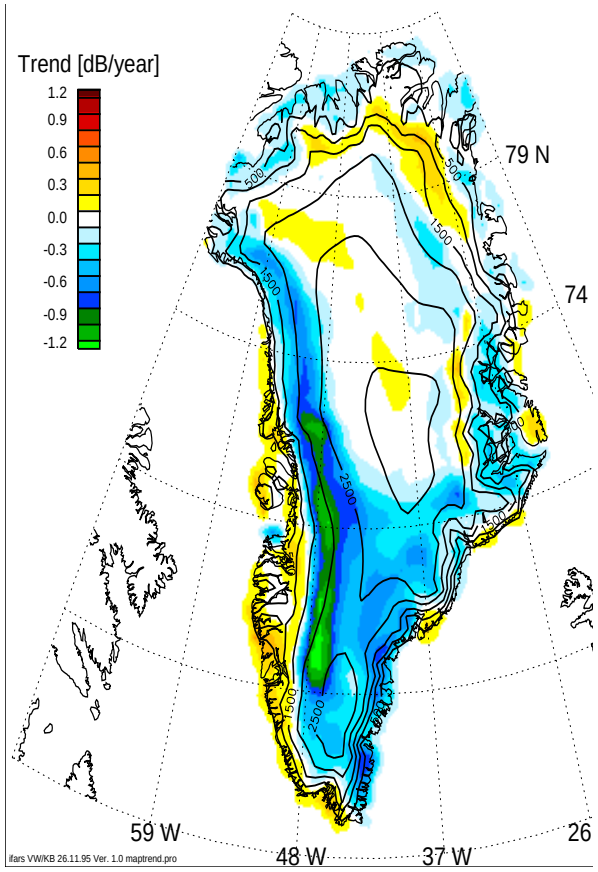


Fig. 7: Temporal backscattering stability measured by the ERS scatterometers over Greenland

## RADARSAT-1 RESULTS

Fig. 8 is a time history of RADARSAT-1 data at HH-polarization over the Amazon for the first 20000 orbits. It is a composite of over 400 data takes from the 16 single beams classes which are plotted as individual colours. The area studied roughly bounded by: 66.5°W, 68.5 °W, and 6.0 °S and 8.0 °S. Each point represents the spatial average of the data used to monitor the antenna pattern, calibrated using the best knowledge of the system and antenna gains and corrected for any S/C roll. The error bars represent the standard deviation of 512 azimuth averages across the swath. The history spans four calendar years. It is difficult to observe any cyclical trend in these results or dependency on beam type.

Fig. 9 is a histogram of the constituent data represented in the ensemble of the points shown in Fig. 7. The mean and standard deviation of the data are indicated. We note that although the mean is close to the ERS-1/2 VV scatterometer, there is considerably more variation. This cannot be due to speckle as each estimate includes many thousands of individual measurements. The absolute levels in each case are determined from precision transponder data [21].

### RADARSAT-1 Instrumental Stability

The question of spatial and temporal stability of RADARSAT-1 can be partially answered from statistics of the internal and external calibration data for the instrument. The error budget for individual measurements is discussed in [22]. Fig. 10 shows a time series from the calibration measurements from precision transponders. Following the analysis done on the ERS SAR [23], we plot the *DGCF* for the four precision transponders used for RADARSAT-1 in Fig. 9 where the RMS variation is 0.42 dB. Assuming the transponders themselves [22] have a radiometric RMS variation of 0.25 dB, we can assess the RMS stability of RADARSAT itself to be less than 0.34 dB since this number includes analysis and processing uncertainty.

Combining this number with the observations over the Amazon (including instrumental variation) shown in Fig. 8, we obtain a RMS variation for the Amazon alone of 0.60 dB.

## ERS-2 SAR RESULTS

There are no routine ERS-2 SAR calibration measurements of the Brazilian rainforest as the ERS-2 SAR calibration is performed using the ESA transponders located in the Netherlands (see paragraph on ERS SAR stability). The Amazon rainforest is only used to derive the antenna pattern [5]. For the purpose of this paper, we have analyzed a set of ten ERS SAR PRI images covering an area of the Amazon rainforest which corresponds to the frame used to derive the antenna pattern, located in Brazil and centered at 7.25° S and 67.43° W. The images were acquired by ERS-2 between April 1996 and April 1999 and processed at the German Processing Facility and at ESA/ESRIN.

Each point in Fig 11 represents the mean $\gamma$ of a PRI image (100 × 100 km), while the error bars show the standard deviation of the azimuth averaged profiles for each image. The $\gamma$ values were obtained using the ERS SAR Toolbox [24].

The measurements in Fig. 11 confirm the temporal radiometric stability of the rainforest in C-band. They also show the high stability of the ERS-2 SAR instrument as the standard variation of the $\gamma$ values is 0.23 dB comparable to those obtained with the transponders measurements. Note that two images have a higher $\gamma$ values which cannot be explained by a visual examination of the images. The temporal standard deviation of $\gamma$ without these two images is 0.06 dB. The $\gamma$ range profiles of the images are flat, confirming the model shown in Fig. 2.

The $\gamma$ measurements of Fig. 11 are however slightly higher than those obtained from the ERS-2 scatterometer and RADARSAT (by about 0.2 dB). Although they fall within the distribution envelope of each of the above data sets, the ERS SAR dataset might not be large enough to adequately represent the statistics for three years and more ERS SAR images should be analyzed before making final conclusions.

## ERS-2 SAR Stability

Fig. 12 gives the time series of three ESA transponder measurements for the ERS-2 SAR since 1995. The overall RMS variation of the DGCF is 0.28 dB with a bias of 0.17 dB against the nominal calibration constant of 59.75 dB. This variation arises from a temporal stability due to a combined SAR and transponder stability and from a spatial stability due to variations within a scene caused by the SAR processor and measurement of the transponder total power. Examination of data from simultaneous pairs and triplets of the transponders located in the Flevoland gives a spatial RMS stability of 0.19 dB. Assuming that the temporal and spatial stabilities are independent, then the temporal RMS stability is 0.21 dB. Included in this temporal stability is the transponder RMS stability; this is estimated [25] to be approximately 0.08 dB.

Combining the uncertainties from the Amazon and transponder data suggest that the rainforest RMS variation is small although a larger Amazon data set is required to adequately access its value.

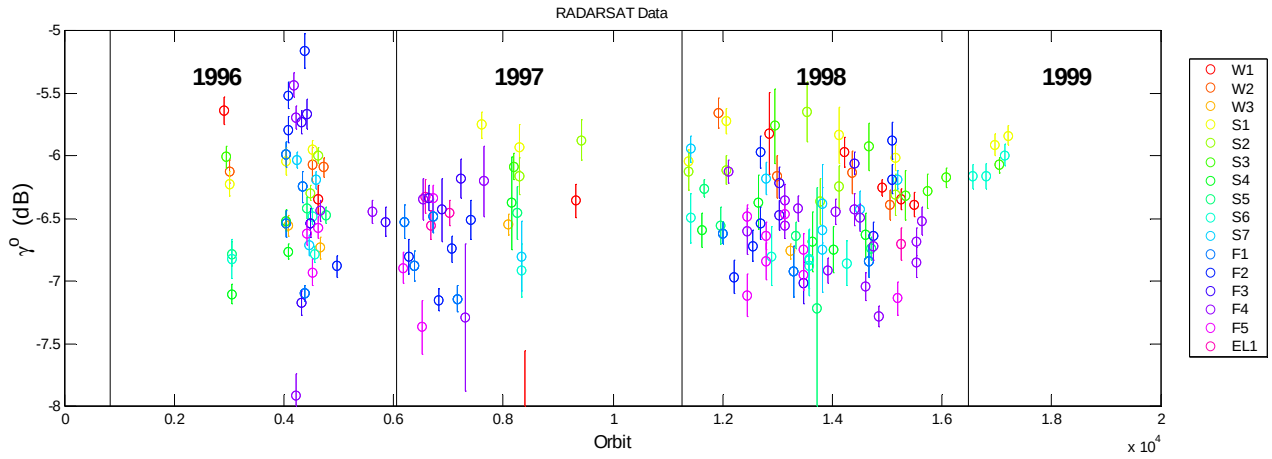


Fig. 8: History of $\gamma$ measurements from RADARSAT-1. The colours represent different single beam results and the error bars the standard deviations of the scene distributions.

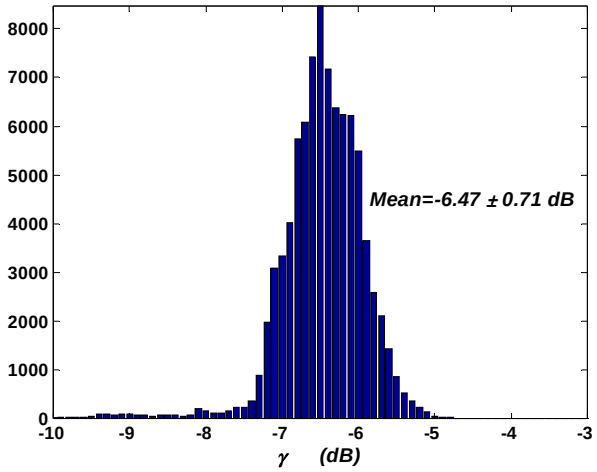


Fig. 9: Distribution of $\gamma$ from RADARSAT-1

## DISCUSSION AND CONCLUSIONS

In this study, we have tried to present a clear picture of the observations of the Amazon rainforest obtained from ERS and RADARSAT together with independent measurements of the respective instrument stabilities. The region is important from many perspectives; however, the aspect emphasized here is the stability of the region as a standard for calibration of spaceborne radars. The validity of property (1) has been unchallenged in making antenna pattern estimates for these instruments over limited angular ranges and is indeed corroborated by transponder measurements taken

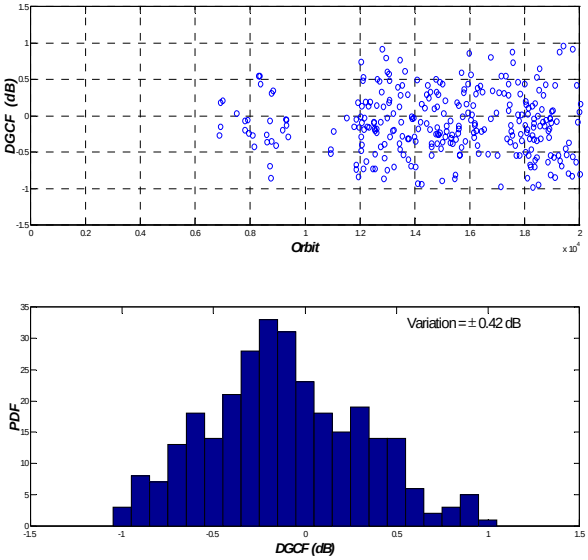


Fig. 10: RADARSAT-1 stability from CSA transponders

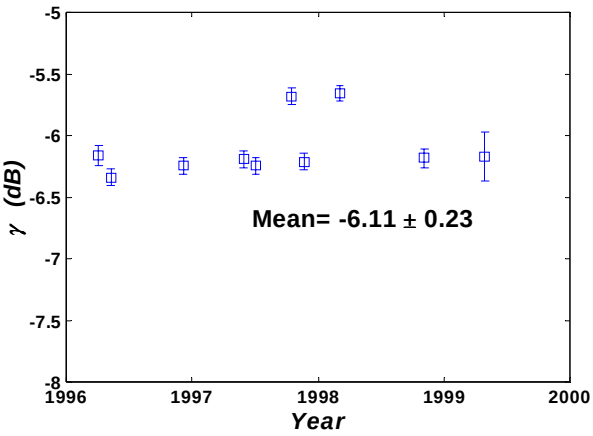


Fig: 11: ERS-2 SAR results from Amazon rainforest

with both ERS and RADARSAT within the limitations of their calibration.

Because the stability of the Amazon measurements is high, it is difficult to separate variations in backscatter measurements from those of the measuring instrument; however, we have been able to demonstrate that on average, each of the instruments has more inherent stability than individual measurements from the Amazon.

In Table 2, we summarize the observed long term backscatter and calibration variations discussed in this study. Where these are available (ERS-2 SAR only), we have computed the constituent parts of the calibration

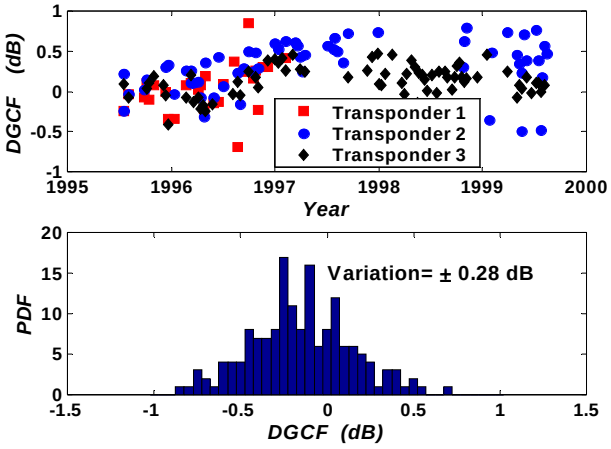


Fig. 12: ERS-2 SAR stability from ESA transponders

due to instrument and calibrator together with analysis. We need to stress that these results are from long term measurements from area samples all greater than $10^4$ $km^2$ and time period greater than 1 year.

Individual measurements may vary considerably from the mean spatial and temporal averages represented in Table 2 and care must be taken in extrapolating results from the longer term/wider area to particular data sets which can be influenced by local precipitation and ground conditions.

The use of Amazon rainforest results for spacecraft mission calibration therefore needs to be confined to those cases where sufficient data samples have been analyzed to assess the variation and associated uncertainty. Otherwise, precision calibrators appear to be the best absolute standard.

Table 2: Long term summary statistics from Amazon rainforest and instrumental calibration

| **RMS Variation** | **SPACEBORNE INSTRUMENT** | | |
|---|---|---|---|
| | **ERS Scatterometer** | **ERS-2 SAR** | **RADARSAT** |
| | **(dB)** | **(dB)** | **(dB)** |
| Rainforest + Instrument | 0.59 | 0.23 | 0.72 |
| Calibrator + Instrument + analysis | 0.20 | 0.28 | 0.42 |
| Calibrator + analysis | NA | 0.19 | NA |
| Instrument | NA | 0.21 | NA |
| Rainforest alone | 0.56 | 0.10 | 0.60 |


ACKNOWLEDGEMENTS

We thank Kevin Murnaghan and Andrew Wind (CCRS), Bob Banik and Marko Adamovic (CSA) in the preparing the data for this document. The cooperation *of RADARSAT International* is also appreciated. Robert Landry and Frank Ahern supplied the J-ERS-1 mosaic of the Amazon. We would also like to acknowledge the cooperation of Henri Laur in facilitating data acquisition and Harry Jackson for his sharing of his intimate knowledge of the ERS transponders. Comments by Joost van der Sanden and Andrew Wind were very helpful in reviewing the manuscript.


REFERENCES


1 JJ van der Sanden, *Radar Remote Sensing To Support Tropical Forest Management*, PhD thesis, Wageningen Agriculture University, Tropenbos-Guyana Programme, 1997, 330p.

2 IJ Birrer *et al.*, "$\sigma^o$ Signature of the amazon rain forest obtained from the Seasat scatterometer," *IEEE GSRS*, GE-20, No. 1, 1992, pp. 11-17.

3 RK Raney, *et al.*, "A plea for radar brightness," *Proc. IGARSS'94*, vol. II, 1994, pp. 1090-1092.

4 DG Long and GB Skouson, "Calibration of spaceborne scatterometers using tropical rain forests," *IEEE GSRS*, vol. 34, 1996, pp 413-424.

5 Laycock, J.E. & Laur, H., "ERS-1 SAR Antenna Pattern Estimation", ESA/ESRIN, ES-TN-DPE-OM-JL01, Issue 1, Rev. 1, September 1994, 32p.

6 K Murnaghan, RK Hawkins, and TI Lukowski, "Combination procedure for RADARSAT antenna generation," *Proc. of 20th Canadian Symposium on Remote Sensing*, Calgary, Alberta, 1998, 6p.

7 Y Fang and RK Moore, "Inflight vertical antenna patterns for SIR-C from Amazon rain-forest observations," *Remote Sens. Environ*, vol. 5, 1997, pp. 407-414.

8 M Shimada and A Freeman, "A technique for measurement of spaceborne antenna patterns using distributed targets," *IEEE GSRS*, vol. 33, 1995, pp. 100-114.

9 South America JERS-1 SAR mosaic courtesy STA/NASDA, made available as a contribution to the CEOS/IGOS-P pilot project "Global Observation of Forest Cover".

10 EPW Attema and FT Ulaby, "Vegetation modelled as a water cloud," *Radio Science*, vol. 13, no. 2 1978, pp. 1299-1307.

11 P Lecomte, “The ERS scatterometer instrument and the on-ground processing of its data,” in *SP-424: Proceedings of a joint ESA-Eumetsat Workshop on Emerging Scatterometer Applications - From Research to Operations*, ESTEC, Nöordwijk, The Netherlands, 5-7 October 1998, pp. 241-260.

12 PCS team, “ERS-2 wind scatterometer cyclic report, from 28th June to 2nd August, Cycle 44,” APP-AEM/PCS/WS99-006, Issue 1, ESA Technical Document, ESRIN, Frascati, Italy, 1999, 31p.

13 A Stoffelen, “Antenna gain variation caused by the sun’s irradiation.” KNMI technical note presented to the ESA Scatterometer Scientific Advisory Group, 1996, 6p.

14 IH Woodhouse, JJ van der Sanden and DH Hoekman, “Scatterometer observations of seasonal backscatter variation over tropical rainforest,” *IEEE TGRS*, vol. 37, 1999, pp. 859-861.

15 P Lecomte and EPW Attema, “Calibration and Validation of the ERS-1 Wind Scatterometer”, in Proceedings First ERS-1 Symposium – Space at the Service of our Environment, Cannes, France, 4-6 Nov, 1992, ESA SP-359, p.19.

16 P Lecomte and W Wagner, “ERS wind scatterometer commissioning and in-flight calibration,” in *SP-424: Proceedings of a joint ESA-Eumetsat Workshop on Emerging Scatterometer Applications - From Research to Operations*, ESTEC, Noordwijk, The Netherlands, 5-7 October 1998, pp. 261-270.

17 H Jackson, (1999) personal communication.

18 PCS team, “ERS-2 wind scatterometer cyclic report, from 19th April to 24th May, Cycle 42,” APP-AEM/PCS/WS99-004, Issue 1, ESA Technical Document, ESRIN, Frascati, Italy, 1999, 42p

19 V Wisman, “A global NRCS database derived from ERS Scatterometer data,” in *Proc of IGARSS’99*, Hamburg , Germany, 1999, pp. 2722-2724.

20 ---, “New views of the earth: Engineering achievements of ERS-1,” ESA SP-1176/III, October 1997, ISBN 92-9092-141-2, p. 41.

21 RK Hawkins *et al.*, “RADARSAT precision transponders”, *Adv. Space Res.*, vol. 19, 1997, pp. 1455-1465.

22 RK Hawkins and SK Srivastava, “Radiometric calibration budget of RADARSAT-1,” this proceedings.

23 PJ Meadows *et al.*, “The ERS SAR performances,” CEOS SAR Workshop, ESA publication WPP-138, 1998, pp. 223-232.

24 ESA, Earthnet Online, , “ERS SAR Toolbox,” http://earth1.esrin.esa.it/STBX

25 H Jackson and A Woode, “Development of the ERS-1 active radar calibration unit,” *IEEE Trans Microwave Theory and Techniques*, 1992, pp. 1063-1069.

| | |
|---|---|
| Filename: | Amazon_1G.doc |
| Directory: | E:\Documents\1999\RADARSAT\Amazon |
| Template: | \\CCRS-NTS1\GroupData\ccrs templates\word\Normal.dot |
| Title: | 1 Introduction |
| Subject: | |
| Author: | CCRS/NRCan |
| Keywords: | |
| Comments: | |
| Creation Date: | 10/15/99 2:16 |
| Change Number: | 10 |
| Last Saved On: | 10/16/99 11:01 |
| Last Saved By: | hawkins |
| Total Editing Time: | 213 Minutes |
| Last Printed On: | 10/16/99 11:53 |

As of Last Complete Printing

| | |
|---|---|
| Number of Pages: | 10 |
| Number of Words: | 2,852 (approx.) |
| Number of Characters: | 16,258 (approx.) |